

Dislocation Models of Crystal Grain Boundaries

W. T. READ AND W. SHOCKLEY
Bell Telephone Laboratories, Murray Hill, New Jersey
 (Received January 9, 1950)

The energies and motions of grain boundaries between two crystallites are investigated theoretically using the dislocation model of grain boundaries. Quantitative predictions made for simple boundaries for cases in which the plane of the boundary contains the axis of relative rotation of the grains appear to agree with available experimental data. The quantitative expression for energy per unit area for small angles is approximately $[Ga/4\pi(1-\sigma)]\theta[A-\ln\theta]$ where G is the rigidity modulus, a the lattice constant, σ Poisson's ratio, θ the relative rotation and A approximately 0.23. Grain boundaries of the form considered may permit intercrystalline slip and may act as stress raisers for the generation of dislocations.

1. DISLOCATION MODEL OF THE GRAIN BOUNDARY

DISLOCATION models of crystal grain boundaries have been proposed by Burgers¹ and by Bragg.² It has recently been shown that these models have certain quantitative consequences which are directly susceptible to experimental tests, so that theoretical and experimental investigations of grain boundaries may furnish evidence for the presence of particular arrays of dislocations in solids.³ Of special interest are grain boundaries between crystallites with a small difference in orientation; we shall show that for these the grain boundary energy can be determined as a function of the angle of misfit and the orientation of the boundary.

The energy of a grain boundary between crystal grains will be a function of the relative orientation of the two grains (this involves three degrees of freedom) and the orientation of the boundary surface itself with respect to the two grains (two additional degrees of freedom). Thus a general grain boundary has five degrees of freedom. It is always possible, at least for small orientation differences, to join the two grains with a suitable array of dislocations lying on the prescribed plane of the grain boundary. We shall not prove this general result here, however, but shall deal in detail with grain boundary models for certain specially simple cases, pointing out how the results may be extended so as to apply more generally.

In particular we shall consider a simple cubic lattice in which the relative rotation of the grains takes place about the z axis and the grain boundary contains the z axis; as a consequence, the problem is two-dimensional, since the situation is independent of z . (Although it is not necessary to introduce screw dislocations, which have components of displacement in the z direction, for the simple cubic lattice, they will be required for body-centered and face-centered cubic lattices, and formulas for their energies are given in Appendix D.) The elasticity theory employed is that for an isotropic

solid and the quantitative results are only approximate except for small angles of misfit, i.e., large spacing between the dislocations. Some features which will arise for large angles are discussed qualitatively in Section 4.

Figure 1 shows the grain boundary for which quantitative calculations have been made. A plane making an angle φ with respect to the x axis is drawn and the two parts of the crystal are each rotated away from the plane by an angle of $\theta/2$. As is seen, some planes from above and from the right must terminate on the boundary, producing dislocations. The numbers of dislocations of the two types per unit length of grain boundary are readily calculated by thinking of the planes as lines of flow. The flux of "y planes" (i.e.,

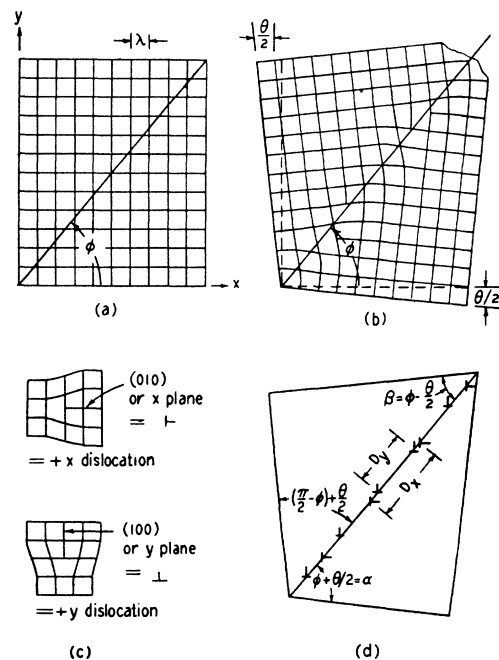


FIG. 1. The dislocation model of a simple grain boundary. (a) Definition of φ , the orientation of the grain boundary. (b) Definition of θ , the angle of misfit. Note that some (100) planes from right (+x planes) and (010) planes from above (+y planes) terminate on the boundary. (c) Symbols for dislocations. (d) Symbolic representation of boundary. *Correction:* The symbol λ should be replaced by a .

¹ J. M. Burgers, Proc. Phys. Soc. **52**, 23 (1940). Proc. Kon. Ned. Akad. V. Wet. Amsterdam **42**, 293 (1939); see also W. G. Burgers, Proc. Kon. Ned. Akad. V. Wet. Amsterdam **50**, 595 (1947).

² W. L. Bragg, Proc. Phys. Soc. **52**, 54 (1940).

³ W. Shockley and W. T. Read, Phys. Rev. **75**, 692 (1949).

$x = \text{constant}$) flowing into the boundary from above is the flux density $(1/a)$ times the cosine of the angle of incidence upon the grain boundary. This leads to a net unbalanced flux per unit length of boundary of

$$\rho_y = \frac{1}{a} (\cos\beta - \cos\alpha) = -\frac{2}{a} \sin\varphi \sin\frac{\theta}{2} \doteq -\frac{\theta \sin\varphi}{a}, \quad (1)$$

where the approximation holds for small values of θ . This is evidently the number of $+y$ dislocations per unit length of boundary. Similar calculations lead to

$$\rho_x = \frac{1}{a} (\sin\alpha - \sin\beta) = -\frac{2}{a} \cos\varphi \sin\frac{\theta}{2} \doteq -\frac{\theta \cos\varphi}{a} \quad (2)$$

for the density of $+x$ dislocations. In applying formulas like these, it is advisable to choose the axes so that $0 \leq \varphi \leq \pi/2$; otherwise difficulties associated with changes in sign of the dislocation types are encountered.

The spacing between dislocations, D_x and D_y , are given by the formulas

$$D_x = \frac{1}{\rho_x} = -\frac{a}{2 \cos\varphi \sin\frac{\theta}{2}} \doteq -\frac{a}{\theta \cos\varphi}, \quad (3)$$

$$D_y = \frac{1}{\rho_y} = -\frac{a}{2 \sin\varphi \sin\frac{\theta}{2}} \doteq -\frac{a}{\theta \sin\varphi}. \quad (4)$$

At distances from the grain boundary larger than D_x and D_y , the crystal will be substantially unstrained. Hence the energy per unit area of the grain boundary will be concentrated near the boundary itself and will be independent of the size of the crystal. These conclusions are verified by the integration of the stress energy which is given in Appendix B.

2. GRAIN BOUNDARY ENERGY

There are three methods of determining the energy of an array of dislocations: (1) Take the volume integral of the strain energy density over the entire body, (2) integrate the work done in producing the state of strain by the surface forces over the *complete boundary*, which includes the surfaces of discontinuity, that is slip planes, (3) determine the work done in creating the dislocations and bringing them together against forces of mutual attraction and repulsion. It can be shown readily that these three methods give the same energy and that the third reduces to the second, which is mathematically simpler than the first, and involves only integrating the shear stress over the slip planes; since the external boundary, being stress-free, gives no contribution to the work and since the relative displacement of the surfaces adjoining the cut is tangential, the work done on a slip plane is one-half the integral of the

tangential, i.e., shearing stress, in the slip direction times the relative displacement, which is constant and equal to one atomic spacing. The factor of one-half comes from the linearity of the stress-strain law. The stresses are determined from an infinite sum of Airy stress functions each representing one dislocation.

For a case like that of Fig. 1, it is convenient to evaluate the stress system due to the x dislocations, denoted by $S(x)$, separately from that of the y dislocations $S(y)$. These stress systems individually give a stress field at large distances from the boundary. However, the combination leads to a stress field localized near the boundary, as discussed in connection with Fig. 1.

The energy is calculated by considering one of the y dislocations and calculating the work done on its slip plane by $S(y)$ and $S(x)$. Each of these energies is simply one-half the lattice constant times the integral of the shearing stress over the slip plane. Although $S(y)$ and $S(x)$ individually give divergent terms, these cancel so that a finite result is obtained. It is found also that the interaction of the y dislocation with $S(x)$ is independent of the relative positions on the boundary of the y dislocation and the set of x dislocations; consequently, the work done is the same for the slip plane of each y dislocation. The same result is true for the x dislocations. The energy of the grain boundary per unit length is then simply the energy per slip plane times the number of slip planes per unit length summed over the two types of slip planes. Since the calculations are made for unit length along the z axis, this gives the energy per unit area of grain boundary.

The formula for the energy per unit area of the grain boundary derived in Appendix B is

$$E = E_0 \theta [A - \ln\theta], \quad (5)$$

where E_0 depends only on the orientation of the grain boundary and the macroscopic elastic constants:

$$E_0 = Ga (\cos\varphi + \sin\varphi) / 4\pi(1-\sigma), \quad (6)$$

where G is the rigidity modulus and σ is Poisson's ratio.* The factor $(\cos\varphi + \sin\varphi)$, which is proportional to the total density of dislocations for a fixed value of θ , is valid only for $0 < \varphi < \pi/2$; within this range it varies by 30 percent.

The quantity A depends upon φ and upon the energy of the atoms at the dislocation itself, where some atoms do not have the correct number of nearest neighbors and the strain lies well out of the Hooke's law range. This energy may conveniently be expressed by a device used in Appendix B, the procedure being summar-

* For an anisotropic material with cubic symmetry and elastic constants c_{11} , c_{12} , c_{44} , the quantity $G/(1-\sigma)$ in (6) is replaced by

$$\frac{c_{44}}{1-\sigma_{100}} \left(\frac{1}{\alpha} \frac{2(1-\sigma_{100})}{1+\alpha(1-2\sigma_{100})} \right)^{\frac{1}{2}}$$

where $\sigma_{100} = c_{12}/(c_{11}+c_{12})$ is Poisson's ratio referred to the crystal axes and $\alpha = 2c_{44}/(c_{11}-c_{12})$ is the anisotropy factor. It is planned to derive this formula in a later paper.

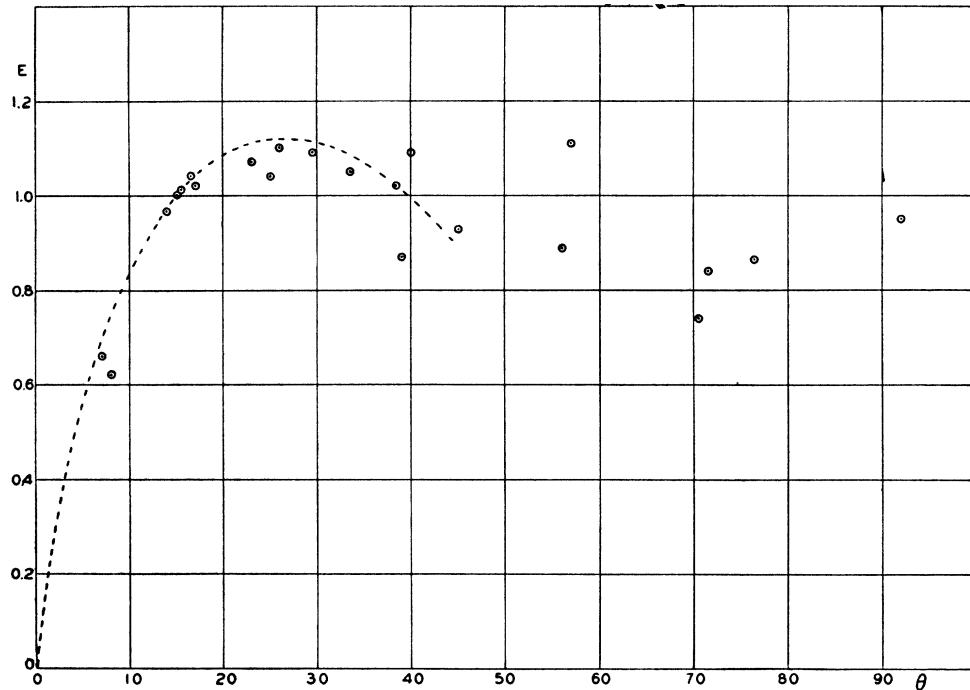


FIG. 2. Energy as a function of θ for grain boundaries. The points show the data of C. G. Dunn for silicon ferrite; see text for orientation. Theoretical curve has $A=0.231$.

ized as follows: The expression for elastic energy density for a single dislocation varies as $(1/r^2)$ from the center of the dislocation and this gives a logarithmic infinity if integrated to $r=0$. Actually it should not be integrated inside of the radius r_l at which the linear Hooke's law breaks down. The energy inside r_l should then be calculated on an atomic basis and added to the elastic energy outside r_l . As is discussed in Appendix B, however, for small angles of misfit precisely the same formula is obtained for the energy if the integration is extended to a radius $r_0 < r_l$ such that the elastic energy calculated for the region $r_l > r > r_0$ has the same value as the correct energy inside r_l . In terms of r_0 defined in this way the value of A is

$$A = A_0 - \frac{\sin 2\varphi}{2} \frac{\sin \varphi \cdot \ln(\sin \varphi) + \cos \varphi \cdot \ln(\cos \varphi)}{\sin \varphi + \cos \varphi} \quad (7)$$

with

$$A_0 = 1 + \ln(a/2\pi r_0). \quad (8)$$

The energy of atomic misfit, which enters through A_0 , occurs in the energy E with factors, given in (5) and (6), which are directly proportional to the total density $\rho_x + \rho_y$ of dislocations. This is to be expected since this highly localized energy should contribute additively.

From (7) $A - A_0$ as a function of φ is seen to be symmetrical about 45° and to vary between $+0.13$ and -0.15 . The maximum A occurs at $\varphi = 6.5^\circ$ or 83.5° and the minimum A at 45° . The curve has a cusp at $\varphi = 0$ or 90° , where $A = A_0$. The variation in A can be neglected at small angles of misfit, where the $-\ln\theta$ -term dominates the energy expression. (But not near the cusps of Section 4.)

Equation (5) will be a good approximation for the energy in a curved boundary if the radius of curvature is large compared to the spacing between dislocations. Letting ds be an element of length of a curved boundary, then the right-hand side of (5) will give dU/ds where U is the energy per unit length in the z direction. Remembering that $|dx| = ds|\cos\varphi|$ and $|dy| = ds|\sin\varphi|$, we then have

$$dU = [Ga/4\pi(1-\sigma)]\theta[A(\varphi) - \ln\theta][|dx| + |dy|].$$

If we can neglect the variation of A with φ , we see that dU is a perfect differential, so that the energy in a segment of boundary connecting two points P and Q will depend only on P and Q , provided that no changes in sign of dx/ds or dy/ds occur along the curve. Thus all boundaries connecting P and Q have the same energy for the same angle of misfit of adjoining grains. Actually there will be a slight preference for a 45° boundary since this gives the minimum A .

The quantity r_0 may be determined by using several approximate but not very accurate methods of estimating the energy in a single dislocation inside the radius r_l . Using Nabarro's⁴ result for a pair of dislocations in a simple cubic model, we calculate that $A_0 = 0.8$. This estimate is not considered very reliable since it depends on the assumption that the interaction between two planes of atoms is based on a sine law of stress and strain.⁵ Another estimate of A_0 is obtained from the requirement that the energy vanish when the dislocations are close enough together to produce an angle of

⁴ F. R. N. Nabarro, Proc. Phys. Soc. London LIX, 256 (1947).

⁵ It is shown that a sine law fails except over a narrow range of angles; see W. M. Lormer, Proc. Roy. Soc. A196, 135 (1949).

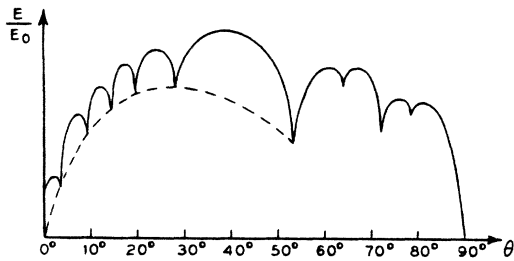


FIG. 3. Energy versus θ for $\varphi=0$ grain boundary showing twin boundary cusp at 53° and fine structure.

misfit of 90° . This leads for $\varphi=0$ to $A_0=\ln\pi/2=0.45$. However, this estimate is also unreliable since it involves the extension of the formula to large angles where the approximations used in its derivation are no longer valid.

3. QUANTITATIVE PREDICTIONS

Fortunately, quantitative conclusions can be drawn from the theory which do not involve the value of A_0 . The first of these is related to Eq. (3) which gives the spacing between dislocations. These spacings are large enough for small angles θ so as to be within the resolving power of light and electron microscopes. We are not aware of any electron-microscope observations of suitable grain boundaries; however, it is very probable that the spacings predicted from (3) have been observed by P. Lacombe in connection with "veining" in aluminum.⁶ Lacombe observes that in a single crystal grain there are faint lines or veins which are revealed as rows of separated etch pits under suitable etching conditions. He has also observed that there are small differences in orientation between the regions separated by the veins. We have proposed that each etch pit originates at a dislocation, where the free energy of the stressed material will be somewhat higher than elsewhere; the pit then grows to large size so that it is observed optically.³ No attempt has been made to calculate the spacings on the basis of a detailed dislocation model for the actual orientation observed; however, the general order of magnitude for the angles of 10^{-3} radians or less and the spacings of 3×10^{-4} cm or less are in agreement with (3) when a reasonable value for a is used.⁷ The behavior of the veins observed by Lacombe is, in other respects, entirely in keeping with the idea that they are widely spaced arrays of dislocations: Under heat treatment they shift to radically different patterns, a result in keeping with the disloca-

⁶ P. Lacombe, Report of Conference on Strength of Solids (The Physical Society of London, 1948). Similar small angle grain boundaries have recently been observed by R. Castaing and A. Guinier in an aluminum-copper alloy. *Comptes Rendus* **228**, 2033 (1949) and *La Recherche Aeronatique* No. 13, 3 (1950).

⁷ We are indebted to Professor Lacombe for confirming, in a personal communication, the conjecture of reference 3 that the data studied there corresponded to a large angle for one specimen and a large spacing for the other. Professor Lacombe indicates that the quantitative aspects of his observations are probably in agreement with (3).

cation proposal. In samples 0.2 cm thick, the vein patterns on the two opposite sides are in register to about $\pm 2 \times 10^{-3}$ cm, the mesh size in the vein pattern being about 2×10^{-2} cm. This suggests that the veins represent cylindrical surfaces and are built up of parallel elements which run perpendicularly (within $2 \times 10^{-3}/2 \times 10^{-1} = 10^{-2}$ radians) through the crystal. Again this is just the behavior expected for an array of dislocations, which must either close on themselves or terminate on a surface. The dislocations in such an array would be under tension and would be perpendicular to the free surface.

The second quantitative conclusion has to do with the energies of grain boundaries and depends only on the energy where strains are small and linear elasticity theory applies. The theory predicts that measured values of grain boundary energy plotted as a function of θ could be fitted by a curve of the form (5), the parameter E_0 being determined without approximations by linear elasticity theory.

Recently C. G. Dunn⁸ has measured grain boundary energies on a relative scale as a function of difference in orientation, θ . Dunn's values of φ are not given, it being assumed that orientation of the grain boundary has a small effect. The specimens used were silicon iron (iron with 3.5 weight percent silicon, body centered cubic), with the (110) plane in the plane of the specimen. The

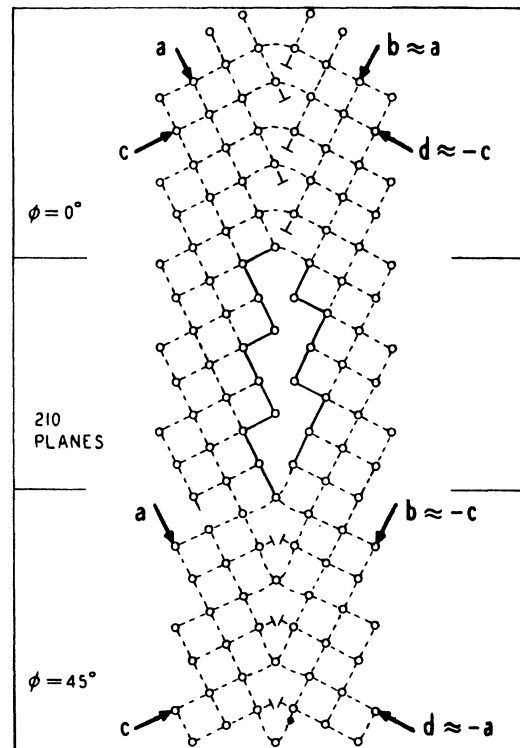


FIG. 4. Grain boundary for twinning on (210) plane showing $\varphi=0$ and $\varphi=45^\circ$ interpretations.

⁸ C. G. Dunn and F. Lionetti, *Trans. A.I.M.E.* **185**, 125 (1949).

grain boundary was made as close as possible to perpendicular to the plane of the specimen and the angle of misfit measured between the $[001]$ directions in the two grains. Viewed in the plane of the specimen the atoms are not arranged in a square lattice but in a rectangular lattice, one side being $\sqrt{2}$ times the other. Consequently, $\theta=180^\circ$ is equivalent to $\theta=0^\circ$; $\theta=90^\circ$ constituting a considerable misfit. Dunn's data in relative units are plotted in Fig. 2. The plot has three striking features: a rapid rise of energy with increasing θ in the range 0° to 15° , a maximum and relatively constant energy in the range 20° to 30° , and a dip at about 70° . The first feature is predicted by the theoretical curve, Eq. (5), which has an infinite slope at $\theta=0$. The position of the maximum of the theoretical curve depends on A , the best fit to Dunn's data being given by $A=0.231$, which is the order of magnitude of the estimates. The theoretical curve is shown in Fig. 2 to 45° and is seen to fit the data surprisingly well even at large angles—a result which suggests that compensating errors may cause (5) to be valid over a larger range than is justified by its derivation. We shall return to the dips at 39° and 70° in the next section.

Dislocation models for grain boundaries in the common crystal lattices would involve screw components and possibly half-dislocations and extended dislocations.⁹ However, it is not considered worth while to

formulate a better theory until energies are measured on an absolute scale for small angle grain boundaries. If such measurements were available, particular dislocation models could be tested by plotting the measured E/θ vs. $\log\theta$. Then according to Eq. (5) the experimental points should fall on a straight line¹⁰ of slope E_0 . The value of E_0 can be calculated without approximations and depends only on the known constants of the material and the particular dislocation model assumed. An agreement between the calculated and measured values would constitute strong evidence for the dislocation model.

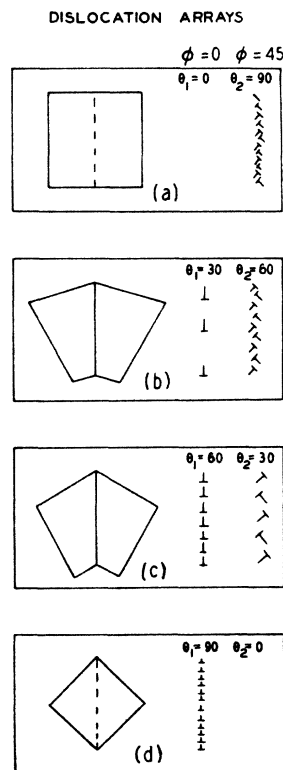
4. LARGE ANGLE GRAIN BOUNDARY

In this section we shall consider certain general features relating to grain boundaries for large angles θ , the remarks still being restricted to the simple cubic model and to values of φ of 0° and 45° unless otherwise stated.

Equation (5) was derived on the assumption that the spacing of dislocations was uniform for all values of θ . Actually this can only be the case when the spacing determined by relations (3) and (4) is an integral number of lattice constants; that is, dislocations must be separated by an integral number of atomic planes. For instance, if θ corresponds to an average spacing of $3\frac{1}{2}$ planes the actual spacing will be irregular, alternating between 3 and 4. As a result the energy is not a smoothly varying function of angle but instead has a number of sharp minima or cusps. We shall show that these cusps are of the $\theta \ln\theta$ form already discussed for $\theta=0$. A plot of E vs. θ showing the more important cusps is given in Fig. 3. The deep cusp in the middle corresponds to a boundary separating twins on the (210) plane. The dashed curve corresponds to (5) and (6). The maxima are treated in Appendix C. There will also be minor cusps between those shown and additional fine cusps for less than 10° .

We shall consider first the reason that cusps are necessary at small values of θ . For $\varphi=90^\circ$ and $\theta=9.4^\circ$, $+y$ dislocations will be required once in every 6 horizontal planes and no x dislocation would be required. For a small increase of $\delta\theta$ in θ from 9.4° , however, dislocations will be required somewhat closer so that occasionally a dislocation will be spaced by 5 planes rather than 6. Where this occurs, it will contribute, at large distances from the grain boundary, the same effect as adding $(1/6)$ of a $+y$ dislocation at each location of a "five" spacing. For small values of $\delta\theta$, these "five" spacings will occur approximately at a spacing of $a/6\delta\theta$. For small values of $\delta\theta$ and large spacings, the energy due to the stress field of these dislocations will come from regions far from the grain boundary and will contribute a term of the order $-(E_0/6)\delta\theta \ln\delta\theta$, since the effective strength of the perturbations is $a/6$.

FIG. 5. Comparison of two models for symmetrical grain boundaries.



⁹ R. D. Heidenreich and W. Shockley, Report of a Conference on Strength of Solids (The Physical Society of London, 1948), page 57.

¹⁰ It is shown in reference 3 that Dunn's data plotted in this way are well fitted by a straight line—the zero intercept of the line giving A .

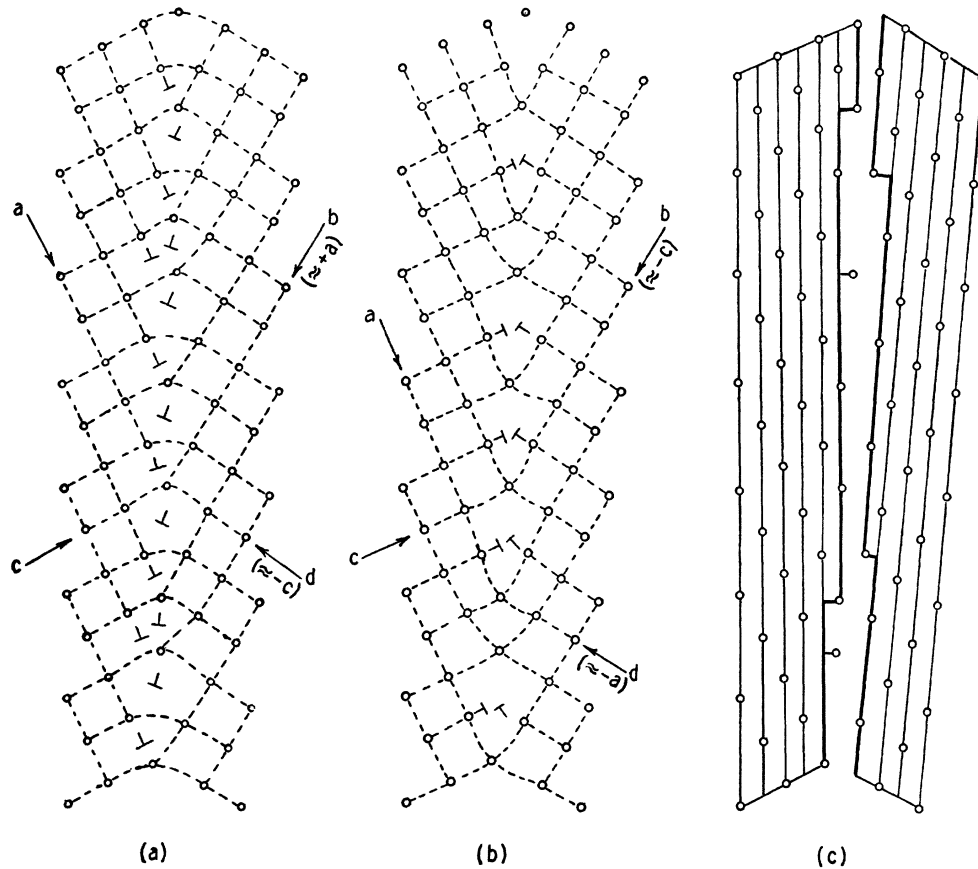


FIG. 6. 60° boundary showing equivalence of $\varphi=0$ and $\varphi=45^\circ$ models and relationship to imperfect (210) surfaces.

A similar $-\delta\theta \ln\delta\theta$ cusp will occur whenever the dislocations are spaced at integral numbers of planes. In addition minor cusps will occur at spacings such as 5.5; because for such a spacing there will be a regular alternation of five and six intervals and a deviation from this, which would require two five spacings to be adjacent, would add a perturbation corresponding to $a/(5+6) = a/11$. This process will obviously continue indefinitely with the conclusion that the E vs. θ -curve has cusps at all values of θ which give rational values for the ratio of dislocations to slip planes across the grain boundary.

From a practical viewpoint the extreme fine structure just discussed will be of no interest and will be smoothed out by statistical fluctuations except for the larger cusps. The most important of these occurs at $\theta = 53^\circ$, corresponding to twinning across the (210) plane. Figure 4 shows the arrangement of the atoms in this case. The heavy lines represent (210) plane boundaries and the bicrystal may be considered as made up by bringing two grains with these (210) faces into contact.

This twin boundary may be described as made up of arrays of dislocations in either of two ways as shown in Fig. 5. We may start with a model with $\varphi=0$ and increase the angle θ_1 between (010) planes up to 53° , at which point $\tan\theta_1/2 = \frac{1}{2}$, corresponding to the twin orientation. If θ_1 is increased to 90° , the grain boundary

should disappear as shown in Fig. 5(d). On the other hand, we can start back from 5(d) with $\varphi=45^\circ$ and produce the same series of orientations. Thus for a given orientation of the grains and the grain boundary, two prescriptions can be given for arrays of dislocations which will join the grains. We shall next investigate the difference between these two prescriptions. The conclusion, reached in the following paragraphs, is that the same arrangement of the atoms can be described as either a $\varphi=0$ boundary or a $\varphi=45^\circ$ boundary and, consequently, that two descriptions are really equivalent.

There may, however, be several atomic arrangements which will accomplish the same joining. In Fig. 4, the plane of the grain boundary is a reflection plane between the two grains. A very similar arrangement may be produced by making the grain boundary a glide plane of symmetry. The relative stability of the two structures will depend upon the detailed nature of the interatomic forces. For whatever structure is the most stable, however, the equivalence of the $\varphi=0$ and $\varphi=45^\circ$ models will be true and the dependence of energy upon small deviations of θ and φ from the twin values will be as described below.

In Fig. 4 in the upper part a set of dotted lines and dislocation symbols are shown; these have been constructed in accordance with the $\varphi=0$ model. In terms

of flow lines this interpretation of the atomic arrangement can be described by writing

$$\varphi=0; \quad c \leftrightarrow -d; \quad a \leftrightarrow b,$$

meaning that the c planes running in at the left are thought of as continuing as $-d$ planes to the right and that a and b planes are to be considered as representing the same set in the undistorted crystal. This leads to a density of dislocations of $\rho_a + \rho_b$ where the ρ 's are the flux density of plane lines into the boundary. Precisely the same atomic arrangement can be described by the arrangement of dislocations shown in the lower part of Figure 4 according to the scheme

$$\varphi=45^\circ; \quad a \leftrightarrow -d; \quad b \leftrightarrow -c,$$

meaning that the a planes are to be considered as continuations of $-d$ and b as $-c$. The density of dislocations for the $\varphi=45^\circ$ model is seen to be

$$\begin{aligned} \rho_c - \rho_b & \text{ for } c\text{-dislocations} \\ \rho_d - \rho_a & \text{ for } d\text{-dislocations.} \end{aligned}$$

Combining these leads to a total number of dislocations $(\rho_d + \rho_c) - (\rho_a + \rho_b) = 2(\rho_c - \rho_a)$, since by symmetry $\rho_d = \rho_c$ and $\rho_a = \rho_b$. For the angle shown $\rho_c = 2\rho_a = 2/a(5)^\frac{1}{2}$ and both models give a density of dislocations equal to ρ_c .

Now let $\theta_1 = 90 - \theta_2$ deviate slightly from 53° , for example, by increasing to 60° , as shown in Fig. 6a. The density of a and b dislocations will increase for the $\varphi=0$ model so that there will be on the average more than one dislocation per plane of set c striking the boundary. These extra dislocations will give rise to a cusp in the energy curve about the twin angle. We shall next show that for this case also the $\varphi=0$ and $\varphi=45^\circ$ models are equivalent and shall evaluate the effective strength of the added dislocations which produce the cusp. For the $\varphi=45^\circ$ model, the density of dislocations decreases as θ_1 increases from 53° to 60° ; consequently there will be less than one dislocation per plane of set c striking the boundary, Fig. 6(b). We shall show algebraically that the number of c -planes having extra dislocations according to the $\varphi=0^\circ$ model just equals the number of c -planes lacking a dislocation according to the $\varphi=45^\circ$ model, and we shall then show geometrically that these two descriptions actually describe the same atomic arrangement.

According to the $\varphi=0^\circ$ model, the density of dislocations is $2\rho_a$ and the excess compared to the density of c -planes is thus $2\rho_a - \rho_c$. According to the $\varphi=45^\circ$ model, the density of dislocations is $2(\rho_c - \rho_a)$ and the excess of c -planes compared to this is $\rho_c - 2(\rho_c - \rho_a) = 2\rho_a - \rho_c$; this is the algebraic proof. Figure 6(a) shows the 60° boundary with dotted lines joining atoms according to the $\varphi=0^\circ$ dislocation model. In Fig. 6(b) the atoms are joined according to the $\varphi=45^\circ$ model. By observing the difference between the two models of the same atomic arrangement in the vicinity of a perturbation, or region where according to the $\varphi=0^\circ$

model two vertical rows end on the same plane, we see that each pair of $a-b$ dislocations on the same c -plane in the $\varphi=0$ model is equivalent to a missing $c-d$ pair on the same plane in the $\varphi=45^\circ$ model. Although both dislocation models represent the same arrangement of atoms, the model consisting of the fewer dislocations is to be preferred on physical grounds as giving the better method of joining the grains, since the number of atoms per plane having a missing bond is equal to the number of dislocations.

In Fig. 6(c) we show the two surfaces which would be formed if the 60° bicrystal were to be pulled apart. It is seen that these are nearly perfect (210) planes except for steps occurring at the perturbations. These steps correspond to an offset of one (210) plane spacing on each grain or a net normal displacement of two plane spacings. Thus the perturbations are equivalent to dislocations of magnitude $2a/(5)^\frac{1}{2}$ with the slip vector perpendicular to the grain boundary. Hence the cusp will have the form of

$$[2/(5)^\frac{1}{2}]E_0(\varphi=0)\delta\theta(A_1 - \ln\delta\theta)$$

by analogy with the $\varphi=0$ calculation which has a similar dislocation array but with strength a . The value of A_1 will be determined by the atomic misfit on the twin boundary and will be different from A_0 .

Probably the most significant feature of the above calculation is that for small angles of deviation the energy of the twin boundary will increase with angle almost as fast [i.e., $2/(5)^\frac{1}{2} = 0.89$] due to the $-\delta\theta \ln\delta\theta$ -term as for a small angle grain boundary.

It is also evident from the general reasoning presented here that similar effects will be produced by varying φ . If the orientation of the two grains is maintained at 53° and the value of φ is changed from 0, the energy will increase as $-\varphi \ln\varphi$ with a coefficient again nearly equal to E_0 .

This last prediction of dependence of energy upon φ is in agreement with the observation of Lacombe¹¹ that when two grains are separated by a boundary consisting in part of a straight twin plane and in part of curved boundary not along the twin plane, the etch used will attack the curved boundary but not the plane boundary, thus showing that large differences in energy are produced by changes in orientation of the grain boundary for the same orientation of the grains.

The dips in Dunn's data of Fig. 2 appear to correspond to expected cusps for the orientation of his crystal. It was seen in Section 3 that, when projected in the plane of the specimen (110), the lattice structure is rectangular with an edge ratio of $1:\sqrt{2}$. The angle θ is measured between [001] directions (short edges). If θ_1 is the angle between the grain boundary and the [001] axis of the first grain, the unit normal to the grain boundary is seen to have components $\cos\theta_1 \cos 45^\circ$, $\cos\theta_1 \sin 45^\circ$, $\sin\theta_1$. A similar result holds for the second

¹¹ Report of a Conference on Strength of Solids, University of Bristol (July 1947) published by the Physical Society, 1948.

grain which makes an angle $\theta_2 = \theta - \theta_1$ with the boundary. In the symmetrical case $\theta_1 = \theta_2 = \theta/2$.

Low energy cusps occur when the two crystals are in register on the same atom at regular intervals of a few lattice constants. The condition that the boundary go through lattice points in the first grain is $\tan\theta_1 = na_y/ma_x$, where m and n are integers and the atomic spacings a_y and a_x in the plane of the specimen are related by $a_y = \sqrt{2}a_x$. The corresponding condition for the second grain is $\tan\theta_2 = \sqrt{2}q/p$, and the two grains will be in register on the same atom at regular intervals along the boundary when the integers m, n, p, q are related by $m^2 + 2n^2 = p^2 + 2q^2 = \text{square of distance between common lattice points, the lattice constant } a_x \text{ in the } [001] \text{ direction being taken as the unit of length. The grain boundary is the } (m, m, 2n) \text{ plane in one crystal and the } (p, p, 2q) \text{ plane in the other.}$

The most important cusps in energy as a function of angle of misfit and orientation of the grain boundary correspond to the shortest intervals between common lattice points; for example, when $m = n = p = q = 1$ the grains are in register on every atom on the boundary and we have a (112) twin, the angle being $\theta = 109.4^\circ$. This angle is not in the range of Fig. 2; however, Dunn has recently¹² obtained a value of 0.22 for the energy on the scale of Fig. 2.

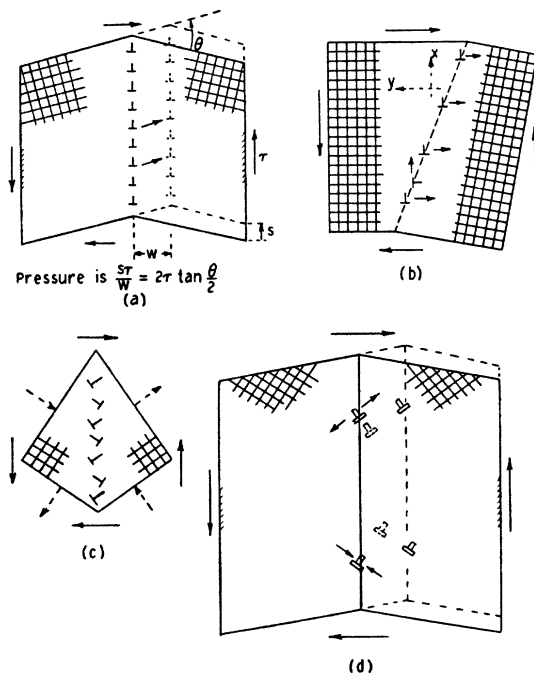


FIG. 7. Mechanism for slip across a grain boundary. (a) Yielding of a symmetrical bicrystal with $\varphi=0$ grain boundary to external shear by sidewise motion of boundary. (b) Separation of x and y arrays on an unsymmetrical boundary by applied shear. (c) Stress applied to bicrystal with 45° grain boundary resulting in (d) sidewise displacement of grain boundary by motion perpendicular to slip planes of dislocations, permitting crystal to yield to applied stress.

¹² Dunn, Daniels, and Bolton, "On the measurement of relative interface energies in twin related crystals," *Trans. A.I.M.E.* **188**, 368 (1950).

The prominent dip in the experimental data near 70° is explained by the fact that the two most important low energy configurations in the range of Fig. 2 both occur at $\theta = 70.6^\circ$. One of these configurations is a symmetrical (111) grain boundary with common lattice points spaced at 2.45 lattice constants; the other configuration is unsymmetrical and involves the coincidence of the (110) plane of one grain with the (114) plane of the other, with points of good fit spaced at intervals of three lattice constants. By comparing the arrangement of atoms on the boundary for the (112) and (111) twins it can be seen¹³ that the former gives the better fit, in agreement with the lower measured energy.

In the range of Fig. 2 the third and fourth cusps in order of increasing distance between common lattice points would be expected at 50° and 87° , respectively, where no experimental points were taken. The fifth cusp occurs at a symmetrical (221) boundary, where the crystals are in register at intervals of 4.25 lattice constants and the angle is 39° . This explains the low point and scatter in the experimental data at this angle, the scatter at cusp angles being attributed to the variation in grain boundary orientation since the energy at a cusp increases at an infinite rate with deviations in either angle of misfit or boundary orientation.

The 20 percent discrepancy between the points at 56° and 57° , which are not cusp angles, has a different origin. The relative energies were calculated from a minimum energy principle involving the equilibrium of surface tensions at the intersection of three grain boundaries, it being assumed that energy depends principally on angle of misfit and that the effect of grain boundary orientation could be neglected.⁸ However, when one boundary is near an energy cusp the derivative of energy with respect to orientation is large and its neglect introduces an error into the calculation of the relative energy of the other two boundaries. The points at 56° and 57° were obtained from the two specimens containing the low energy boundaries with θ near the 70.6° cusp. In Appendix F this point is discussed in detail and the energy *vs.* angle relations are derived for three intersecting grains taking account of the dependence of energy on boundary orientation.

The general behavior of the energy *vs.* angle curve appears to be in qualitative agreement with the extensive system of observations made by C. S. Smith¹⁴ of grain boundary angles. In his study the angles where three grain boundaries run together were measured on polished sections of polycrystalline samples and the statistical distribution of observed angles was studied. Even if all grain boundaries had the same energy, so that the three dihedral angles about the common grain edge would each be 120° , the metallographic section would

¹³ C. S. Barrett, *Structure of Metals* (McGraw-Hill Book Company, Inc., New York, 1943), p. 315.

¹⁴ C. S. Smith, "Grains, phases and interfaces: An interpretation of microstructure, A.I.M.M.E. Technical Publication No. 2387, Class E, Metals Tech. (June, 1948).

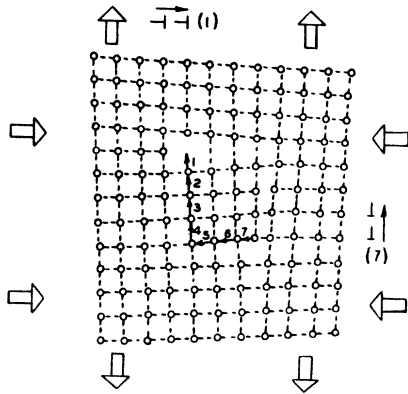


FIG. 8. Motion of dislocations perpendicular to slip planes produced by diffusion of atoms.

introduce a statistical fluctuation in observed angles. Smith found that the statistics of the observed angles were consistent, or at least not strikingly inconsistent, with a single interfacial energy for the boundaries. This at first seems to contradict the predictions made here that the grain boundary energy fluctuates violently and that, as indicated in Fig. 2, energies of less than half the average should occur in about 15 percent of the cases; the impression gained from Fig. 2 is erroneous, however, because it shows the energy as a function of one angle only. If any of the three angles which specify relative orientation of the grains is large, a relatively large grain boundary energy will be obtained. If we assume that the grain boundary energy for a general orientation is the sum of three functions like that of Fig. 2, one for each angle, then we estimate that energies less than 50 percent of the average will be obtained in only about 3 percent of the cases. Consequently, observations of grain boundaries for grains selected at random would show such a small percentage of low energy boundaries that their presence would have only a slight effect on the statistics.

5. DYNAMICS OF THE GRAIN BOUNDARY MODEL

The dislocation model of the grain boundary appears to have the potentiality of giving the "viscous grain boundary" behavior studied extensively by Zener and Kê.¹⁵ Two separate mechanisms are involved in shear across the grain boundary, corresponding to motion of the dislocations in their slip planes and motion perpendicular to the slip planes. (The latter involves diffusion of atoms in a way which we shall shortly illustrate in Fig. 8.)

The two basic processes are shown in Fig. 7. A boundary with $\varphi=0$ is shown and the bicrystal is cut so that the largest faces are parallel to the boundary. If a shear stress τ is applied as shown, the dislocations tend to slide on the slip planes in the direction of the dotted

positions. In Appendix A we show that the force acting on a unit length of a dislocation under these conditions is simply τa , so that the pressure on the grain boundary is $\tau a/D_y \doteq \tau\theta$. The same pressure is derived by considering the deformation of the crystal. If we imagine the left grain to be held fixed, then the work done when the boundary moves a distance W is $S\tau$ per unit area, so that the pressure is $S\tau/W = \tau 2 \tan \frac{1}{2}\theta = \tau\theta$ for small angles. This type of motion can thus permit relative shear of the two crystals to take place across the grain boundary.

Figure 7(a), however, is a very special case. A more typical situation is shown in (b). Here there are two

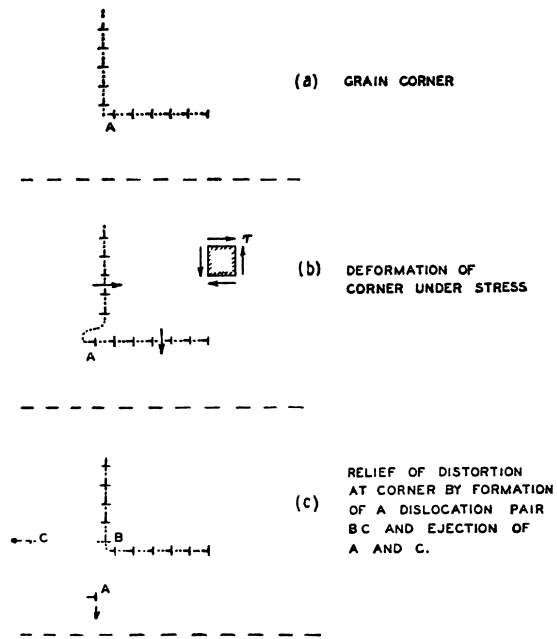


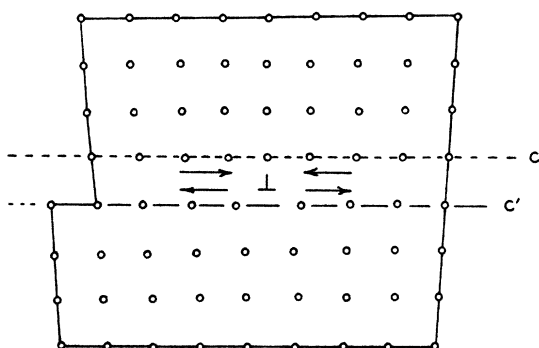
FIG. 9. Formation of a dislocation pair at a grain corner under applied stress.

sets of dislocations and in this case if we move the grain boundary to the right, by sliding the x dislocations to the right and the $-y$ dislocations down, no net shearing motion of the crystal results. The reason for this is that the prescription of dislocations of Eqs. (3) and (4) is just that necessary to permit the two grains to join with a fixed relative orientation; a proof of this statement is given in Appendix E. The difference between (b) and (a) is connected with the limiting behavior as $\varphi \rightarrow 0$. As φ becomes very small, the spacing D_y is given by $a/\theta\varphi$. Thus $D_y \rightarrow \infty$ as $\varphi \rightarrow 0$. As the boundary moves to the right a distance W , however, the $-y$ dislocations move a distance W/φ so that each y plane is cut by $(W/\varphi)/D_y = W\theta/a$ dislocations of y type as it moves. Each of these produces an offset " a " giving a shearing motion of $W\theta$. Inspection shows that the sign of this shear just cancels the $W\theta$ term due to the motion shown in (a). Thus no net shear is produced by motion of the boundary while any $-y$ dislocations are present.

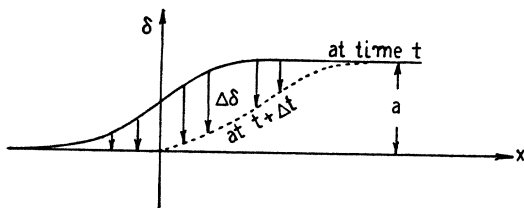
¹⁵ C. Zener, *Elasticity and Anelasticity of Metals* (University of Chicago Press, Chicago, 1948); T. S. Kê, *J. App. Phys.* **20**, 274 (1949).

If a shearing stress is applied to (b), the dislocations try to slip as shown by the arrows. As a result the x and y sets pull apart until the increasing elastic energy of the material between them balances the applied stress. If the angle φ is small, this will result in curvature of the dense line of dislocations and resultant high stress values. We shall return to the high stresses later in this section in connection with grain boundaries as stress raisers.

The processes which may follow the development of the stressed situation in (b) are illustrated in a simpler form in (c) and (d). Here we show a $\varphi = 45^\circ$ boundary with a shearing stress system which develops no shear in the slip planes. The shear stress system is equivalent to a normal stress system shown as dotted arrows. These stresses tend to squeeze out (or pull in) the extra half-planes of atoms. The mechanism whereby this may be accomplished will be discussed below; however, if we assume that the squeezing out actually occurs, then the motion of the dislocations will be as shown in (d). Here we consider two dislocations on a grain boundary which divides the specimen in two; actually there will be many dislocations on the boundary. The normal stresses on the half-planes cause one to shorten and the other to lengthen, moving the dislocations to the dotted positions. The dotted positions, however, corre-



(a)



(b)

FIG. 10. The force on a dislocation. (a) Single dislocation in a cubic crystal, showing shearing stresses on planes C and C' . (b) Plot of δ = difference in displacement on C and C' at times t and $t + \Delta t$.

spond to a relative motion of the arrays of the two types of dislocations; and in order to keep the grain boundary in a minimum energy condition, the dislocations will slip in their own planes so as to move to positions in the dotted grain boundary which are at the same height as their original positions. These combined motions produce a net horizontal motion of the grain boundary in which no dislocations cut the (110) planes which are parallel to the top and bottom of the figure. The result is thus a yielding to the shear of amount $S = W/2 \tan\theta/2$ as for Fig. 7(a).

The process which can produce motion perpendicular to the slip plane is shown in Fig. 8, which corresponds to 7(d) turned through 45° . We suppose vacancy diffusion takes place, the process being initiated by jump (1) in the figure which permits the half-plane to grow by one atom, a vacancy being produced next to the advancing edge. This vacancy diffuses until it is filled by jump 7 which shortens the other dislocation by one atom on the leading edge of the half-plane.

The shear produced across a general small angle grain boundary will be a mixture of effects like those considered in (a) and (c). For large angle grain boundaries, such as are dealt with in most experiments, the density of dislocations will be so high and the possibilities of alternative descriptions so many that other approaches may be better such as those of Mott¹⁶ and Kê,¹⁷ which consider the boundary to be a mixture of good fit and bad fit. However, the feature discussed in Fig. 8 has one consequence in agreement with experiment: The mechanism involved is that of self-diffusion and, consequently, the activation energy for the process will be the same as that for self-diffusion, in agreement with the findings of Kê for aluminum, α -brass and α -iron.¹⁸

Even for small angle grain boundaries, however, the theory discussed in connection with Fig. 7 is oversimplified because it neglects the effects of screw components of the dislocations and the possibility of half-dislocations.¹⁹ The screw components are discussed in Appendix D and are seen to exert forces like those of charged wires on each other. These forces will tend to stabilize the dislocation arrays.

The pressure on a grain boundary suggests a mechanism for the creation of dislocation pairs in the interior of polycrystals. As mentioned earlier, an applied shearing stress tends to pull the boundary apart, creating regions of stress concentration. We now show how the distortion of a grain corner under stress could lead to the formation of a dislocation pair at the corner. Consider the right-angle corner illustrated in Fig. 9(a), where the grain in the upper right-hand quadrant is disoriented by a small clockwise rotation relative to the adjoining material. The grain boundary is symmetrical

¹⁶ N. F. Mott, Proc. Phys. Soc. London **60**, 391 (1948).

¹⁷ T. S. Kê, J. App. Phys. **20**, 274 (1949).

¹⁸ T. S. Kê, Phys. Rev. **73**, 267 (1948).

¹⁹ R. D. Heidenreich and W. Shockley, Report of a Conference on Strength of Solids (Physical Society, London, 1948), p. 57.

and runs along the $+y$ and $+x$ axes, which are rows of $+y$ and $-x$ dislocations respectively. When an external shearing stress is applied as shown in (b) the y dislocations are pushed to the right and the $-x$ dislocations are forced downward. The entire pressure on the grain boundary and the forces on the dislocations are held in equilibrium by the corner, which alone prevents the relative displacement of the two segments of the boundary. The corner is thus a region of high strain, the strain energy per unit applied stress being proportional to the area of the boundary and the density of dislocations. As the applied stress is increased, the relative displacement of the two rows of dislocations increases until the distortion of the corner is so severe, as shown in Fig. 9(b), that it is easier energetically to form a dislocation pair BC , Fig. 9(c), where B fills the gap on the grain boundary and A and C are ejected and move under the applied stress to the external surface, thus contributing to the observed slip of the specimen.

In conclusion it may be pointed out that the idea of pressure on a grain boundary due to applied stresses constitutes a prediction from dislocation theory that grain boundaries, and similarly veins like those observed by Lacombe, should displace in a particular way under the influence of applied stress.

The authors would like to express their gratitude for suggestions and encouragement in connection with this research to J. H. Hollomon, C. S. Smith, W. G. Burgers, C. G. Dunn and C. Herring. We are also indebted to Mrs. G. V. Smith and Miss D. T. Angell for computations and other assistance in preparing the manuscript.

APPENDIX A

The Force on a Dislocation

When a dislocation moves under the action of an external stress field, work is done on the boundary by the applied forces. Some of this work goes into increasing the energy of distortion of the crystal and is recoverable, and the remainder is dissipated at the dislocation as heat or acoustical waves. Defining the force on a dislocation as the energy dissipated in moving the dislocation through unit distance on the slip plane, we show, first by an intuitive example and then by a careful analysis of the physical phenomena, that the force per unit length on a line dislocation is the lattice constant times the applied shearing stress in the slip direction.

In the simple example, Fig. 10, let the dislocation move a distance L from one side of a crystal to the other, producing a relative tangential displacement of the upper surface through one lattice constant a . Letting τ be the applied stress on the slip plane the work done is τaL . The elastic energy of distortion in the two parts of the crystal above and below the slip plane is the same before and after slip, so that all of the work has gone into heat. Since an amount of heat τaL has been produced in moving the dislocation through a distance L , it would be reasonable to assume that the force on the dislocation was τa .²⁰ We shall find by a more thorough analysis that this semi-intuitive result is correct.

If we assume that inertial effects can be neglected, then the energy dissipated is equal to the external work done minus the

²⁰ This reasoning is very similar to that of N. F. Mott and F. R. N. Nabarro, Report of a Conference on Strength of Solids (The Physical Society, London, 1948), p. 1.

change in stored energy of distortion. The rate of change of internal energy is equal to the rate at which surface stresses are doing work on the complete boundary of the crystal, which includes not only the external boundary but the internal surfaces of discontinuity, or slip planes. Thus the stored energy is the sum of the external work and the work done on the slip planes—from which it follows that the energy dissipated is the negative of the work done on the slip planes.

Now consider a single dislocation in a cubic lattice, Fig. 10. Let C and C' be the atomic planes adjoining the slip plane. The shearing stresses on C and C' are shown in the figure. Superposed on this anti-symmetrical shear distribution we have the shear stress due to the external field. Figure 10(b) is an approximate plot of the discontinuity in displacement δ across the slip plane, the atoms being in register at the extreme right and offset by one lattice spacing at the left, with a transition region of a few atomic spacings at the dislocation. The dotted curve shows the discontinuity in displacement at a time Δt later, when the dislocation has moved a distance Δx . Clearly the limit $\Delta\delta/\Delta t$ is a symmetrical function of distance x along the slip plane. The rate of doing work on the slip plane is the integral of the shearing stress times the rate of relative displacement $\Delta\delta/\Delta t$ of the planes C and C' . Since the latter is symmetrical, the anti-symmetrical shear distribution due to the dislocation itself gives no contribution, and we have for the rate of energy dissipation

$$\frac{\tau}{\Delta t} \int_c \Delta\delta dx,$$

where τ is the external shear stress, which may be considered constant over the atomic dimension involved, and the integral is the area between the two curves in Fig. 10(b) which is readily seen to be $a\Delta x$. Thus, taking account of signs, the energy dissipated in moving the dislocation a distance Δx is $\tau a\Delta x$ and the force on the dislocation is τa .²¹

In this derivation it has been assumed for simplicity that the slip vector is at right angles to the axis of the dislocation. However, this restriction is readily seen to be unnecessary. In the general case the force on a dislocation is τa where τ is the shearing stress in the slip direction and a is the magnitude of the slip vector or lattice spacing in the slip direction. Thus the result derived applies to dislocations with screw components, which are generally required in an actual face-centered or body-centered cubic lattice.

APPENDIX B

Derivation of the Energy vs. Angle Formula

The shear stress τ_{xy} due to a single $+y$ dislocation located at the origin of the coordinate system is²² where for convenience lengths are expressed in units of " a " and stresses in units of $G/[2\pi(1-\sigma)]$. The shearing stress due to an infinite row of dislocations, Fig. 1, spaced at a distance D_y along the line inclined at an angle φ to the x axis is

$$\sum_{n=-\infty}^{\infty} \frac{x_n(x_n^2 - y_n^2)}{(x_n^2 + y_n^2)^2}, \quad (\text{B.2})$$

where

$$\begin{aligned} x_n &= x + nD_y \cos \varphi \\ y_n &= y + nD_y \sin \varphi. \end{aligned}$$

²¹ It may be noted that this differs by a factor of $\pi(1-\sigma)$ from the result computed by J. S. Koehler using linear isotropic two-dimensional elasticity theory (Phys. Rev. **60**, 400 (1941)). This may be attributed to the fact that Koehler does not take account of the work done by the surface forces.

²² J. S. Koehler, Phys. Rev. **60**, 397 (1941).

$$\tau_{xy} = \frac{x(x^2 - y^2)}{(x^2 + y^2)^2} \quad (\text{B.1})$$

From (3) and (4) of Section 1, D_x and D_y are given by

$$\begin{aligned} D_x &= a/(\theta \cos \varphi) \\ D_y &= a/(\theta \sin \varphi). \end{aligned} \quad (\text{B.3})$$

The infinite sum (B.2) is readily transformed to

$$\sum_{n=-\infty}^{\infty} \frac{\partial}{\partial y} \left(\frac{y_n}{2} \right) \left[\frac{1}{x_n + iy_n} + \frac{1}{x_n - iy_n} \right].$$

Using the complex variable $z = x + iy$ and the complex constant $z_1 = D_y e^{i\varphi}$ and letting Re mean "real part of," this becomes

$$\text{Re} \sum_{n=-\infty}^{\infty} \frac{\partial}{\partial y} \left(\frac{y + nD_y \sin \varphi}{z + nz_1} \right).$$

Multiplying numerator and denominator by $z - nz_1$ and adding a constant term which vanishes in the differentiation, we have

$$\text{Re} \sum_{n=-\infty}^{\infty} \frac{\partial}{\partial y} \left[\frac{(y + nD_y \sin \varphi)(z - nz_1)}{z^2 - n^2 z_1^2} - \frac{D_y \sin \varphi}{z_1} \right].$$

Since the terms with n odd cancel in pairs, this can be expressed in the form

$$\text{Re} \frac{\partial}{\partial y} \left[\frac{z_1 y - z D_y \sin \varphi}{z_1} \right] \sum_{n=-\infty}^{\infty} \frac{z}{z^2 - n^2 z_1^2}.$$

The sum of the infinite series is known and is equal to

$$(\pi/z_1) \cot(\pi z/z_1).^{23}$$

This gives

$$\text{Re} \left[\frac{\pi}{z_1^2} \frac{\partial}{\partial y} (z_1 y - z D_y \sin \varphi) \cot \frac{\pi z}{z_1} \right] \quad (\text{B.4})$$

for the stress caused by the infinite set of $+y$ dislocations. Putting this in the form

$$\text{Re} \left\{ \frac{\pi}{z_1^2} \left[D_y \cos \varphi \cot \frac{\pi z}{z_1} - i(z_1 y - z D_y \sin \varphi) \frac{\pi}{z_1} \csc^2 \frac{\pi z}{z_1} \right] \right\}, \quad (\text{B.5})$$

we see that at an infinite distance from the line of dislocations, where $z = Nz_1$ and $N \rightarrow \infty$, the stress approaches $(\pi/D_y) \cos \varphi \sin 2\varphi$. A similar analysis for the dislocations with vertical slip planes gives a stress at infinity of $-(\pi/D_x) \sin \varphi \sin 2\varphi$. From (B.3) we see that the sum of these is zero, so that the shear stress at infinity vanishes as required.²⁴

We shall now calculate the self- and interaction energies of the two sets of dislocations.

The work of interaction on the vertical slip plane of one of the $+x$ dislocations is found by integrating the shear stress (B.4) due to the set of $+y$ dislocations, the integration being taken from x, y to $x, y+R$ where R is very large and x and y are the coordinates of the $+x$ dislocation, with the origin at a $+y$ dislocation. Making use of the fact that the equation of the grain boundary is $y = x \tan \varphi$, the integral of (B.4) with respect to y gives

$$-(\pi R/2D_y) \cos \varphi \sin 2\varphi \quad (\text{B.6})$$

for all points on the boundary. Thus the interaction energy is the same for all the $+x$ dislocations. In the same way the work of interaction on the horizontal slip plane of a $+y$ dislocation is

²³ E. P. Adams, *Smithsonian Mathematical Formulae and Tables of Elliptical Functions*, p. 129, No. 6.495, Smithsonian Institute, Washington, D. C. (1922).

²⁴ From (B.5) it is seen that the stress due to the $+y$ dislocations does not vanish except when $\sin 4\varphi = 0$ or $z = z_1/2$. Thus in the general case there is a net force on the $+x$ dislocations and the assumed dislocation array is not in equilibrium. However, near the boundary a small change in position corresponds to a relatively large change in stress, so that equilibrium could be satisfied by a slight rearrangement of dislocations involving a deviation of the boundary from a straight line. This would have little effect on the stress energy at distances from the boundary comparable to the spacing between dislocations and therefore would not appreciably affect the calculated energy.

found to be

$$-(\pi R/2D_x) \sin \varphi \sin 2\varphi \quad (\text{B.7})$$

and is the same for all the $+y$ dislocations.²⁵

Since the self-energy per $+y$ dislocation is obviously the same for each dislocation, we consider the dislocation at the origin, where $y=0$, and integrate the shearing stress (B.5) due to the $+y$ dislocations from $x=r_0$ to $x=R$, where r_0 is the radius of a small circle around the dislocation and, as previously explained, is a parameter determined by the local energy of misfit which must be calculated on an atomic basis. This integration gives for the self-energy per $+y$ dislocation

$$\frac{1}{2} \left[\frac{\pi R}{D_y} \sin 2\varphi \cos \varphi - \ln \left(\frac{2\pi r_0}{D_y} \right) + \sin^2 \varphi \right]. \quad (\text{B.8})$$

It can be seen that varying r_0 changes the energy by a constant amount, independently of the orientation of the adjoining crystals. Thus adjusting r_0 is equivalent to adding the energy of local atomic misfit to the angle dependent energy of the surrounding field. This is a valid procedure provided the angle of misfit is small enough that the local energy of atomic misfit is not dependent on the spacing between dislocations.

The self-energy of the set of $+x$ dislocations is found in the same way to be

$$\frac{1}{2} \left[\frac{\pi R}{D_x} \sin \varphi \sin 2\varphi - \ln \left(\frac{2\pi r_0}{D_x} \right) + \cos^2 \varphi \right] \quad (\text{B.9})$$

per dislocation.

The work done on a horizontal slip plane is (B.7)+(B.8) equals

$$\frac{\pi}{2} R \sin 2\varphi \left[\frac{\cos \varphi}{D_y} - \frac{\sin \varphi}{D_x} \right] - \frac{1}{2} \left[\ln \left(\frac{2\pi r_0}{e D_y} \right) + \cos^2 \varphi \right], \quad (\text{B.10})$$

where e is the base of the natural logarithms. The relationships between D_y , D_x , and φ which caused the stress to vanish at ∞ in (B.5) causes the coefficient of R to vanish so that the energy is convergent.

The energy per unit length of boundary is found by dividing the work done on a slip plane by the spacing between slip planes. This gives [(B.7)+(B.8)]/ D_y for the $+y$ dislocations, and [(B.6)+(B.9)]/ D_x for the $+x$ dislocations. The sum of these is

$$\frac{1}{2} \left[\frac{\cos^2 \varphi}{D_y} + \frac{\sin^2 \varphi}{D_x} - \frac{1}{D_y} \ln \left(\frac{2\pi r_0}{e D_y} \right) - \frac{1}{D_x} \ln \left(\frac{2\pi r_0}{e D_x} \right) \right] \quad (\text{B.11})$$

or, using (B.3) the energy E per unit area of the boundary is

$$E = E_0 \theta [A - \ln \theta] \quad (\text{B.12})$$

where E_0 depends only on φ and the constants of the material and is given in dimensional units by

$$E_0 = \frac{Ga}{4\pi(1-\sigma)} (\cos \varphi + \sin \varphi) \quad (\text{B.13})$$

and A depends on r_0 and, therefore, on the energy in the immediate vicinity of the dislocation and is given by

$$A = A_0 - \frac{\sin 2\varphi}{2} - \frac{\sin \varphi \cdot \ln(\sin \varphi) + \cos \varphi \cdot \ln(\cos \varphi)}{\sin \varphi + \cos \varphi} \quad (\text{B.14})$$

where A_0 is the value of A when the boundary is along a crystal axis and is given by

$$A_0 = 1 + \ln[a/(2\pi r_0)]. \quad (\text{B.15})$$

²⁵ The interaction energies per unit area of the grain boundary are, respectively, (B.6)/ D_x and (B.7)/ D_y , and these in general are not equal. However this does not contradict the conservation of energy because these energies represent the work of interaction on the slip planes only; the total interaction energies should include also the work done on the external surfaces by the stresses at infinity, which do not vanish for each set of dislocations individually.

APPENDIX C

Energies of Irregular Arrays

In this Appendix we consider the case of a symmetrical boundary for angles where the spacing of dislocations is not uniform and the energy is not the same for every dislocation. Angles corresponding to average spacings which are simple ratios like 4/3 or 3/2 can be represented by superposing two or more regular arrays of dislocations with different spacings. For instance, the $\varphi=90^\circ$ model for $\theta=41^\circ$ can be represented as the sum of two arrays as follows

$$X X X O X X X O = X O X O X O X O + O X O O O X O O,$$

where X represents a dislocation and O no dislocation and the spacing between the symbols is one plane. The self-energies of the two arrays are readily obtained from Appendix B, since each set alone corresponds to a single boundary with angle of misfit determined by the spacing. To obtain the interaction energy of two regular arrays we determine a general expression for the energy of interaction between a single dislocation on the y axis and a row of dislocations spaced at regular intervals D along the y axis. Taking the origin at one of the dislocations of the regular array, we let $y < D$ be the coordinate of the single dislocation and find the interaction energy as a function of y .

The shear stress due to the regular array is

$$-\operatorname{Re}(\pi x/D) \operatorname{csch}^2(\pi/D)(x+iy).$$

Integrating with respect to x from r_0 , y to R , y where $R \gg D$ gives

$$-\operatorname{Re}[\ln 2 \sinh(\pi/D)(r_0+iy) - (\pi r_0/D) \coth(\pi/D)(r_0+iy)]$$

which reduces to the usual formula when $y=0$. When $y \gg r_0$, we have

$$\ln 2 \sin(\pi y/D).$$

The energy of interaction is therefore negative for $D/6 < y < 5D/6$ and positive in the interval $\pm D/6$ about each dislocation of the regular array, the distribution being symmetrical about the minimum energy $-\ln 2$ at $y=D/2$.

For the 41° boundary the interaction energy per unit length for the set spaced at $2a$ is $-\frac{1}{4} \ln 2$. This can be checked by comparing with the interaction energy per unit length for the $2a$ spaced set, which is

$$-\frac{1}{4}[\ln 2 \sin(\pi/4) + \ln 2 \sin(3\pi/4)] = -\frac{1}{4} \ln 2,$$

the two interaction energies being equal as required by the reciprocal theorem. Adding the interaction energies to the self-energies gives a total energy of 0.86 as compared with 0.75 given by Eq. (5) on the assumption of a regular spacing of $4a/3$.

For $\theta=37^\circ$ the $\varphi=90^\circ$ model is

$$X X O X X O = X O O X O O + O X O O X O.$$

Here the interaction energy per unit length is $(\frac{1}{3}) \ln 2 \sin(\pi/3)$ for each regular set giving a total energy of 0.83 as compared with 0.73 for a regular spacing of $3a/2$.

APPENDIX D

Energy of Arrays of Screw Dislocations

The screw components give rise to shear stresses τ_{xz} and τ_{yz} acting in the z direction and on both sets of slip planes. There is no interaction between screw and x and y components but the two types of screws interact with one another, since each set of screws gives rise to shear stresses on the slip planes of the other set. Formulas for the self- and interaction energies will be derived and applied to the special case of symmetrical boundaries for both regular and irregular arrays.

The component of displacement w , in the z direction, for a single screw dislocation is given by

$$w = (b/2\pi) \tan^{-1}(y/x), \quad (\text{D.1})$$

where b is the z component of the slip vector. This formula shows

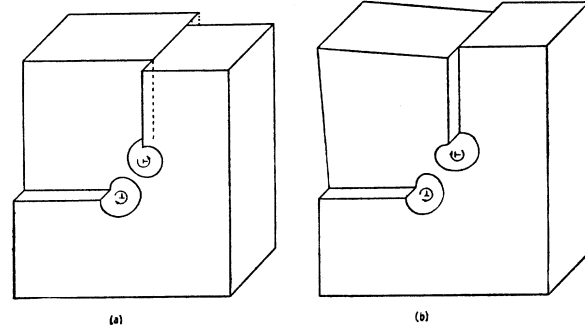


FIG. 11. Interactions between screw dislocations showing that stress fields of unlike dislocations cancel at large distances.

that the elastic behavior of the screw dislocation is the same no matter what slip plane is involved. The stresses due to the dislocation are

$$\begin{aligned} \tau_{yz} &= G \frac{\partial w}{\partial y} = \frac{Gb}{2\pi} \frac{x}{x^2+y^2} \\ \tau_{xz} &= G \frac{\partial w}{\partial x} = \frac{Gb}{2\pi} \frac{-y}{x^2+y^2} \\ \tau_{xy} &= 0. \end{aligned}$$

The calculations of the interaction of screw dislocations is greatly simplified by the fact that one can show a direct correspondence with two-dimensional electrostatic theory. We consider two dislocations with slip vectors b_1 and b_2 and choose two coordinate systems (x_1, y_1) and (x_2, y_2) measured from the dislocations. The energy density in the stress field is then

$$\begin{aligned} &(\frac{1}{2}G)(\tau_{xz}^2 + \tau_{yz}^2) \\ &= \frac{1}{8\pi(4\pi/G)} \left[\frac{(2b_1)^2}{r_1^2} + \frac{(2b_2)^2}{r_2^2} + 2 \frac{2b_1 2b_2}{r_1^2 r_2^2} (x_1 x_2 + y_1 y_2) \right] \\ &= \frac{1}{8\pi\epsilon} [\mathbf{E}_1 + \mathbf{E}_2]^2, \end{aligned}$$

where \mathbf{E}_1 and \mathbf{E}_2 are vectors directed away from the dislocations with magnitudes

$$E_1 = 2b_1/r_1, \quad E_2 = 2b_2/r_2$$

and

$$\epsilon = 4\pi/G.$$

This shows that the energy density is formally the same as that for two wires with charges per unit length of b_1 and b_2 embedded in a medium with dielectric constant ϵ . We may, therefore, use theorems from electrostatics to calculate the energies of arrays of screw dislocations. (The Taylor type of dislocation cannot be represented in this way, because the u and v displacements are not solutions of Laplace's equation $\nabla^2 u = 0$, whereas w is a solution.)

The interaction of two screw dislocations is shown in Fig. 11. It is seen that if the dislocations have opposite signs, their stress fields cancel at distances from them comparable to twice their separations, whereas if they are of the same sign the stress fields add.

The problem of the infinite self-energy of a single dislocation for small distances is again solved by cutting off the integration at such a radius r_0 that the energy inside of the radius at which Hooke's law fails is correctly given. Since the disturbance in a screw dislocation is very different on an atomic scale from that in a Taylor dislocation, the value of r_0 will be different. The same qualitative arguments will apply, however. The use of r_0 corresponds in the electrostatic problem to calculating the energy of charges on the surfaces of hollow cylinders so that the field energy inside the cylinders is negligibly small.

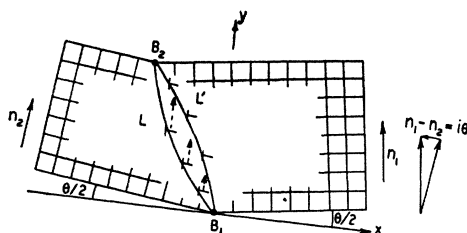


FIG. 12. Displacement of grain boundary by motion of dislocations without relative motion of grains. (y dislocations not shown.)

The potential energy of an array of screw dislocations spaced a distance D apart in a plane will be a minimum when the signs of b alternate corresponding to a grid of alternately charged wires. The potential of such a set of wires must behave as $-(2b/\epsilon) \ln r$ near each plus wire and as $+(2b/\epsilon) \ln r$ near each negative wire. If the wire centers are at $x=0, D, 2D, \dots$, the solution of Laplace's equation which satisfies these requirements and vanishes at large $|y|$ is

$$\text{Real Part of } -(2b/\epsilon) \ln \tan \pi(x+iy)/2D.$$

We shall assume that the dislocations are so far apart that the cylinders of radius r_0 are practically equipotentials; otherwise the approximation that the energies of atomic misfit do not interact is in error. Assuming that, the potential at $x=r_0, y=0$ is

$$-(2b/\epsilon) \ln(\pi r_0 2D).$$

The self-energy per dislocation of the array is $(\frac{1}{2})b$ times this potential and the self-energy per unit area, E_s , is $(1/D)$ times this latter:

$$E_s = \frac{1}{D} \frac{b}{2} (2b/\epsilon) \ln 2D / \pi r_0 = \frac{Gb^2}{4\pi D} \ln 2D / \pi r_0.$$

In many cases it will not be possible to have the simple alternating scheme of screw components used for calculating E_s . For the $\varphi=0$ and $\varphi=45^\circ$ models, the regularity of the spacing makes it possible and in that case a term of form E_s can be added to E . For small angles both terms are of the form $E\theta(A - \ln\theta)$ and their sum is of the same form, the value of E and A depending on the particular relationship of screw to Taylor components.

If screw dislocations are coupled to the x and y dislocations of the boundary of Fig. 1, the interactions between them will be such as to stabilize the position of the x set in respect to the y set. For example, for the $\varphi=45^\circ$ model, there are equal numbers of x and y dislocations. The most stable arrangement will be that which results in a maximum of cancellation of the screws, Fig. 11, just as if one grid of alternately charged wires were placed next to another so that the charges neutralized. Mathematically, this reduces the screw energy to zero. Physically, it means that the dislocations will draw together until non-linear interactions, which are represented by the r_0 terms, become important.

APPENDIX E

A Theorem on the Displacement of Grain Boundaries for Small θ

Consider two grains whose orientation differs by a small angle θ as shown in Fig. 12. Suppose that at two points B_1 and B_2 on the boundary the two crystals are perfectly in register on the same atom. We wish to show that sliding the set of dislocations which compose the boundary to different places on their slip planes, so as to move the boundary to a new position, does not tend to produce relative shear motion of the two grains. To prove this we consider the number of $+x$ dislocations required for the two positions of the boundary, L and L' . If two unit vectors along the cell edges, as shown, are n_1 and n_2 , then the number of $+x$ disloca-

tions will evidently be

$$dS \cdot (n_1 - n_2) / a = -dx \cdot \theta / a$$

for small values of θ . Hence, in order to fit the two grains together with the proper number of $+x$ dislocations, the spacing must be θ/a as projected on the x axis. Since sliding the dislocations on their slip planes does not affect this density, slipping the x dislocations from L to L' still leaves the correct density. The same reasoning may be applied to the y dislocations (not shown on Fig. 12). Furthermore, the points B_1 and B_2 are unchanged and are correctly in register for both the distribution of L and L' . Hence the same set of dislocations are the optimum set for both L and L' and, since both L and L' preserve the registration at B_1 and B_2 , it is evident that shifting the dislocations from L to L' does not produce relative motion of the two grains.

Any method of moving the boundary connecting B_1 and B_2 to a new position leaves the number of required dislocations of each type unchanged for the entire boundary, but only the sliding of each dislocation on its slip plane preserves the correct number for every segment of the boundary, that is, preserves the correct density.

APPENDIX F

Energy vs. Angle Relations for Three Intersecting Boundaries

In this section we obtain the formulas for the energy ratios in a three grain specimen, taking into account the dependence of energy on grain boundary orientation.

Figure 13 shows three grain boundaries intersecting in a line normal to the plane of the drawing at 0. The grain boundary energies are E_1, E_2 , and E_3 , the angles between boundaries are ψ_1, ψ_2 , and ψ_3 , and the average orientations of the boundaries with respect to specified crystal axes in the two adjoining grains are φ_1, φ_2 , and φ_3 .

The energy-angle relations for this case have been derived by C. Herring²⁶ from the minimum energy principle and in the present notation are given by equations of the form

$$E_1 + E_2 \cos \psi_3 + E_3 \cos \psi_2 + \sin \psi_2 (\partial E_3 / \partial \varphi_3) - \sin \psi_3 (\partial E_2 / \partial \varphi_2) = 0, \quad (\text{F.1})$$

where the partial derivatives with respect to boundary orientation are measured in the direction of counterclockwise rotation about the intersection.

Equation (F.1) expresses the vanishing of the first-order change of grain boundary energy due to an infinitesimal displacement of the intersection in the plane of the first boundary, it being assumed that the second and third boundaries acquire angles at points separated from 0 by distances which, although still infinitesimal, are large compared to the displacement of 0. Two other equations of which only one is independent are obtained from (F.1) by

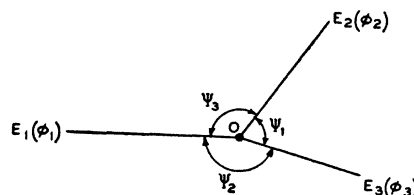


FIG. 13. Three intersecting grain boundaries.

²⁶ C. Herring, "Surface tension as a motivation for sintering," a paper presented at the Symposium on Physics of Powder Metallurgy, organized by Sylvania Electric Products, Inc., Bayside, Long Island, New York (August 24-26, 1949). Plans have been made to publish the papers of this Symposium in book form.

rotation of subscripts. These equations are satisfied by

$$\frac{E_1}{(1+\epsilon_2\epsilon_3)\sin\psi_1+(\epsilon_3-\epsilon_2)\cos\psi_1} = \frac{E_2}{(1+\epsilon_1\epsilon_3)\sin\psi_2+(\epsilon_1-\epsilon_2)\cos\psi_2} \\ = \frac{E_3}{(1+\epsilon_1\epsilon_2)\sin\psi_3+(\epsilon_2-\epsilon_1)\cos\psi_3}, \quad (\text{F.2})$$

where

$$\epsilon_1 = (1/E_1)(\partial E_1/\partial \varphi_1)$$

with similar definitions for ϵ_2 and ϵ_3 . When the ϵ 's vanish (F.2) reduces to the triangle of forces. When any one of the ϵ 's cannot be neglected the triangle of forces gives erroneous values for both of the two independent energy ratios. However if only one boundary, say the first, is near a cusp position so that the other two boundaries have small derivatives with respect to orientation, then (F.1) gives to a good approximation

$$E_1 = -E_2 \cos\psi_3 - E_3 \cos\psi_2, \quad (\text{F.3})$$

where E_2 and E_3 are to be determined from the best fit curve to

data obtained from samples where none of the boundaries are near energy cusps. Applying this procedure to Dunn's two specimens each with one boundary near the 70.6° cusp,²⁷ we obtain 0.77 and 0.78 for the points at 70.5° and 71.5° respectively. As discussed in the text, the triangle of forces gives unreliable values for the energies of the other boundaries in these samples.

For a simple cubic lattice with none of the three boundaries near a cusp position, the ϵ 's can be determined by differentiation of (5) of the text, making use of (6) and (7) for the dependence of E_0 and A on φ . When the variation in A can be neglected, we have

$$\epsilon_1 = \frac{\partial}{\partial \varphi_1} \ln E_0(\varphi_1) = \frac{\cos \varphi_1 - \sin \varphi_1}{\cos \varphi_1 + \sin \varphi_1} = \frac{1 - \tan \varphi_1}{1 + \tan \varphi_1}$$

with similar expressions for ϵ_2 and ϵ_3 . This formula is valid for $0 < \varphi < \pi/2$.

²⁷ C. G. Dunn and F. Lionetti, specimens S10 and S11, reference 8, Table I, p. 128.